atmosphere

Article

Numerical Study on the Urban Ventilation in Regulating Microclimate and Pollutant Dispersion in Urban Street Canyon: A Case Study of Nanjing New Region, China

Fan Liu, Hua Qian *, Xiaohong Zheng, Lun Zhang and Wenqing Liang

School of Energy and Environment, Southeast University, Nanjing 210096, Jiangsu, China; 18252712528@163.com (F.L.); xhzheng@seu.edu.cn (X.Z.); zhanglun@seu.edu.cn (L.Z.); lwq21cn@hotmail.com (W.L.)

* Correspondence: qianh@seu.edu.cn

Received: 30 July 2017; Accepted: 26 August 2017; Published: 29 August 2017

Abstract: Urban ventilation plays an important role in regulating city climate and air quality. A numerical study was conducted to explore the ventilation effectiveness on the microclimate and pollutant removal in the urban street canyon based on the rebuilt Southern New Town region in Nanjing, China. The RNG $k - \varepsilon$ turbulence model in the computational fluid dynamics (CFD) was employed to study the street canyon under parallel and perpendicular wind directions, respectively. Velocity inside of the street canyon and temperature on the building envelopes were obtained. A novel pressure coefficient was defined, and three methods were applied to evaluate the urban ventilation effectiveness. Results revealed that there was little comfort difference for the human body under two ventilation patterns in the street canyon. Air stagnation occurred easily in dense building clusters, especially under the perpendicular wind direction. In addition, large pressure coefficients ($C_P > 1$) appeared at the windward region, contributing to promising ventilation. The air age was introduced to evaluate the "freshness" of the air in the street canyon and illustrated the ventilation effectiveness on the pollutant removal. It was found that the young air distributed where the corresponding ventilation was favorable and the wind speed was large. The results from this study can be useful in further city renovation for the street canyon construction and municipal planning.

Keywords: street canyon; computational fluid dynamics (CFD); ventilation effectiveness; the age of air

---

1. Introduction

The outdoor thermal and wind environment are of great significance to the living conditions and people's daily activities [1]. With the rapid urbanization, street canyons appear in cities as more and more high-rise buildings spring up, resulting in poor city ventilation [2]. Stagnant air caused by poor ventilation in street canyons leads to the massive accumulation of pollutants and anthropogenic heat, exacerbating the outdoor air quality [3–5] and the Urban Heat Island effect (UHI) [6–9]. Outdoor environment is essential not only for people directly exposed to the circumstance [10,11], but it also has an important influence on the indoor environment [12]. From the last decade, study on microclimate in a street canyon has become a hot issue focussing on ventilation, temperature, and pollutant dispersion. Numerical and experimental validation studies on street canyons indicate that ventilation is a vital element in these related indices on urban microclimate [12]. Air in the city can be well mixed and exchanged under the windy condition that introduces the fresh air from the suburbs into the city. The heat and pollutant generated from the city is likely to be removed by the airflow [1]. It is noted that the effectiveness of the heat and pollutant removal is strongly affected by the airflow patterns inside street canyons.

Many studies have been carried out to investigate the airflow pattern around buildings by wind tunnel experiments [13,14] and field measurements [15]. With the development of computer technology and numerical computation, the computational fluid dynamics (CFD) method has been gradually employed attributed to its low expense and high flexibility. Combining the simulation method and the architectural design strategy, it enables architects to better design and evaluate the city wind environment. Studies on outdoor environment by CFD method mainly focus on airflow pattern analysis [16,17], human comfort evaluation at the pedestrian level around buildings [18], and the prediction of pollution dispersion [19]. Over the last few decades, many attempts have been made to link urban ventilation research with the urban design in a given condition. The ventilation has been found to have a close relationship with the building layout, which subsequently affects the air quality in street canyons [20]. Moreover, the canyon aspect ratio and the orientation of street canyons are two crucial parameters informing the urban microclimates and influencing the thermal comfort of pedestrians, which is more obvious in full-scale high-rise deep street canyons [19,21]. The vertical microclimate and mass-exchange have also been investigated in different street canyons with different geometries [22]. It has been noted that the street canyon is a key factor in maintaining urban microclimates by previous studies. The mechanisms of the airflow patterns and the ventilation effectiveness on heat reduction and pollutant dispersion in street canyons have been fully understood. However, only simple construction models [23,24] and a typical wind direction in street canyons [25] are considered in most existing numerical studies. Limited investigations are conducted to study the urban ventilation and its effects on the microclimate. Moreover, qualified indexes for the evaluation of the urban ventilation effectiveness have not been appropriately considered up until now.

To illustrate ventilation effectiveness in cities with street canyons, a numerical study has been carried out in this paper based on the project of Southern New Town region, Nanjing. A long street altered from a military airport runway is centered in this region, with a large number of building clusters including residential areas, innovative, and military districts on both sides. The airflow inside the street canyon and the temperature distribution at building facades were discussed under different local metrological parameters. The ventilation effectiveness was evaluated by three commonly used methods on the heat and pollutant removal. Results from this study can be helpful for further the city construction and urban environment maintenance with urban street valleys.

2. Study Case

The Southern New Town region, located at the southeast Nanjing, is designed to be built on the location of a military airport. The original airport runway will be altered into a long street at the center of this region. Surrounding areas are designed to three particular sub-regions (residential areas, innovative, and military districts) as well as some ecological areas and open space. The long street canyon goes through the region from southeast to northwest, as shown in Figure 1.

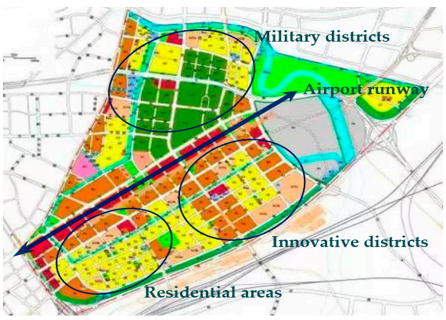

Figure 1. Planning diagram of the Southern New City region.

As planned, the total area is 12.88 km^2, with construction land of 5.93 km^2. The local wind rose diagrams monitored are shown in Figure 2. Table 1 presents the local meteorological parameters, obtained at the height of 10 m above the ground for numerical simulations, such as air temperature, wind velocity, and prevailing direction. The prevailing wind directions are south-southeast with the average speed of 2.4 m/s in summer, and east-northeast with the average speed of 2.7 m/s in winter. Table 2 shows the calorific intensity on the building surface and in the interspaces in summer. These parameters are all used as boundary conditions for simulation scenarios.

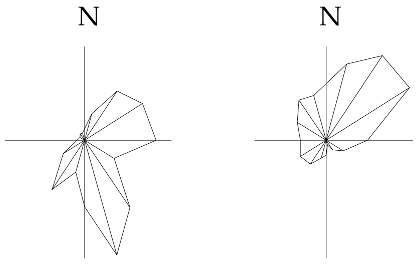

(**a**) (**b**)

Figure 2. Wind rose diagrams of Nanjing: (**a**) Summer; (**b**) Winter.

Table 1. Meteorological data for simulations.

Scenario	Season	Temperature (°C)	Prevailing Wind Direction	Wind Speed (m/s)
1	Summer	20~37	SSE	2.4
2	Winter	−2~10	ENE	2.7

SSE: South-Southeast; ENE: East-Northeast.

Table 2. The calorific intensity in summer.

Items	Military Districts	Innovative Streets	Residential Areas
Building area (m^2)	167.0	410.3	488.4
Body heat (W·m^{-3})	1.6	4.3	4.5
Surface heat (W·m^{-2})	91.3	155.6	147.0

Three commonly used methods are adopted to evaluate the ventilation effectiveness on the heat and pollutant removal, i.e., wind scales and human body comfort, wind pressure, and the age of air. To evaluate the pollutant dispersion in the street canyons, the metric, "local mean age of air" is used in this paper. The local mean age of air was firstly proposed as an indicator of the air quality in indoor spaces [26,27], which has been confirmed to be applicable in outdoors [28,29]. It serves as an indicator of outdoor air quality in this paper to help recognize the stagnant areas or polluted region where contaminants easily accumulate.

3. Computational Settings and Parameters

The Fluent calculation module in the Ansys 17.0 software (ANSYS, Inc., Canonburg, PA, USA) is chosen to conduct the numerical simulations. According to the three-dimensional architectural model of the Southern New Town region, an appropriate computational domain is selected and meshed, and the entire airflow field is solved with mathematical models under corresponding boundary and initial conditions. The wind field, temperature distribution, and pollutant dispersion are calculated and analyzed.

3.1. Geometric Model, Computational Domain and Meshing Generation

It is essential to simplify the geometric model for meshing, reducing computational nodes, and accelerating the convergence speed before calculation. Small convex and concave structures of buildings are neglected, and all curved shapes are regularized in the process. The simplified model is shown in Figure 3. In terms of the size of the computational domain, the top boundary is set as 4 H_{max} (H_{max} is the height of the tallest building), lateral boundaries is set as 5 W (W is the width of the target region), and the inlet and outflow boundaries are set as 6 L (L is the length of the target region).

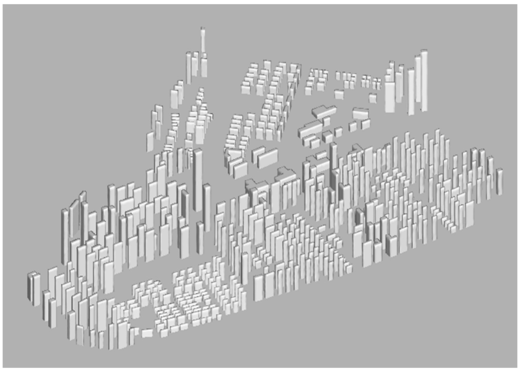

Figure 3. Physical model in computational fluid dynamics (CFD).

In order to predict the airflow around buildings in acceptable accuracy, the most important thing is to correctly reproduce the separating airflows near the corners and the walls. Therefore, a fine grid arrangement is required for calculation. Before the meshing, the whole domain is divided into several connected areas according to construction shapes and sizes. Unstructured tetrahedral cells are used to construct the whole computational domain. For the present simulation, the minimum grid resolution is set to be 0.5–5.0 m ($\frac{1}{10}$ of the building scale [30]) within the target region, and increases gradually with distance above 100 m in the computational domain. The resulting grid contains 7,890,431 control volumes (see Figure 4), and is based on a grid-sensitivity analysis focused on the mean wind speed in the entrance.

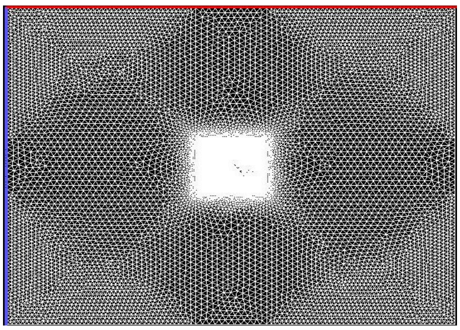

Figure 4. Computational grid on the bottom surface the domain. Total number of cells is 7,890,431.

3.2. Methodology

The outdoor airflow is governed by conservations of mass and momentum in each flow direction. An incompressible tairflow with constant properties is assumed in the numerical calculation. The Reynolds-Averaged Navier-Stokes (RANS) equations are used and written as follows [31].

The mass conservation equation,

$$\mathrm{div}\,\mathbf{U} = 0 \tag{1}$$

The equations for conservation of momentum,

$$\mathrm{div}(U\mathbf{U}) = -\frac{1}{\rho}\frac{\partial P}{\partial x} + \gamma \mathrm{div}(\mathrm{grad}(U)) + \frac{1}{\rho}\left[\frac{\partial\left(-\rho\overline{u'^2}\right)}{\partial x} + \frac{\partial\left(-\rho\overline{u'v'}\right)}{\partial y} + \frac{\partial\left(-\rho\overline{u'w'}\right)}{\partial z}\right] + S_{Mx} \quad (2a)$$

$$\mathrm{div}(V\mathbf{U}) = -\frac{1}{\rho}\frac{\partial P}{\partial y} + \gamma \mathrm{div}(\mathrm{grad}(V)) + \frac{1}{\rho}\left[\frac{\partial\left(-\rho\overline{u'V'}\right)}{\partial x} + \frac{\partial\left(-\rho\overline{v'^2}\right)}{\partial y} + \frac{\partial\left(-\rho\overline{v'w'}\right)}{\partial z}\right] + S_{My} \quad (2b)$$

$$\mathrm{div}(W\mathbf{U}) = -\frac{1}{\rho}\frac{\partial P}{\partial z} + \gamma \mathrm{div}(\mathrm{grad}(W)) + \frac{1}{\rho}\left[\frac{\partial\left(-\rho\overline{u'w'}\right)}{\partial x} + \frac{\partial\left(-\rho\overline{v'w'}\right)}{\partial y} + \frac{\partial\left(-\rho\overline{w'^2}\right)}{\partial z}\right] + S_{Mz} \quad (2c)$$

with three normal stresses,

$$\tau_{xx} = -\rho\overline{u'^2},\ \tau_{yy} = -\rho\overline{v'^2},\ \tau_{zz} = -\rho\overline{w'^2} \quad (3a)$$

and three shear stresses,

$$\tau_{xy} = \tau_{yx} = -\rho\overline{u'v'},\ \tau_{xz} = \tau_{zx} = -\rho\overline{u'w'},\ \tau_{yz} = \tau_{zy} = -\rho\overline{v'w'} \quad (3b)$$

These extra turbulent stresses in Equation (3) are the Reynolds stresses. $S_{Mx} = 0$, $S_{My} = 0$, and $S_{Mz} = -\rho g$ denote projections of the body force in x, y, and z directions, respectively. The density variation is calculated by the Boussinesq approximation, i.e., $\rho = \rho_0[1-\beta(T-T_0)]$.The energy equation,

$$\mathrm{div}(T\mathbf{U}) = \frac{1}{\rho}\mathrm{div}(\alpha \mathrm{grad} T) - \left(\frac{\partial\overline{u't'}}{\partial x} + \frac{\partial\overline{u't'}}{\partial y} + \frac{\partial\overline{u't'}}{\partial z}\right) + S_T \quad (4)$$

where the flow variables $\mathbf{u}$ (hence also u, v, and w), p and t are described by the sum of a mean and fluctuating component, i.e., $\mathbf{u} = \mathbf{U} + \mathbf{u}'$ ($u = U + u'$, $v = V + v'$ and $w = W + w'$), $p = P + p'$, $t = T + t'$. γ is the kinematic viscosity, α the thermal diffusion coefficient, ρ_0 the reference density, T_0 the reference temperature.

Closure is obtained by the Renormalization Group (RNG) $k-\varepsilon$ turbulence model with enhanced wall treatment [32]. The transport equations for turbulent kinetic energy (TKE) k and dissipation rate ε are given as:

$$\mathrm{div}(\rho k\mathbf{U}) = \mathrm{div}(\alpha_k\mu_{eff}\mathrm{grad}k) + \tau_{ij}\cdot S_{ij} - \rho\varepsilon \quad (5)$$

$$\frac{\partial}{\partial x_j}(\rho\varepsilon\mathbf{U}) = \mathrm{div}(\alpha_\varepsilon\mu_{eff}\mathrm{grad}\varepsilon) + C^*_{1\varepsilon}\frac{\varepsilon}{k}\tau_{ij}\cdot S_{ij} - C_{2\varepsilon}\rho\frac{\varepsilon^2}{k} \quad (6)$$

with

$$\tau_{ij} = -\rho\overline{u'_i u'_j} = 2\mu_t S_{ij} - \frac{2}{3}\rho k\delta_{ij},\ S_{ij} = \frac{1}{2}\left(\frac{\partial u_i}{\partial x_j} + \frac{\partial u_j}{\partial x_i}\right) \quad (7)$$

and

$$\mu_{eff} = \mu + \mu_t,\ \mu_t = \rho C_\mu\frac{k^2}{\varepsilon} \quad (8)$$

$$C^*_{1\varepsilon} = C_{1\varepsilon} - \frac{\eta(1-\eta/4.377)}{1+0.012},\ \eta = \frac{k}{\varepsilon}\sqrt{2S_{ij}\cdot S_{ij}} \quad (9)$$

The convention of the suffix notation is that i or j = 1 corresponds to the x-direction, i or j = 2 the y-direction, i or j = 3 the z-direction. μ is the molecular viscosity, μ_t the turbulent viscosity, δ_{ij} the Kronecker delta ($\delta_{ij} = 1$ if $i = j$ and $\delta_{ij} = 0$ if $i \neq j$). $C_\mu = 0.0845$, $\alpha_k = \alpha_\varepsilon = 1.39$, $C_{1\varepsilon} = 1.42$, $C_{2\varepsilon} = 1.68$ [33].

The age of air is utilized to demonstrate the effects of the ventilation corridor on the "freshness" of outdoor air in the Southern New Town region. The definition of the age of air φ_n at a point within a zone is described in Figure 5.

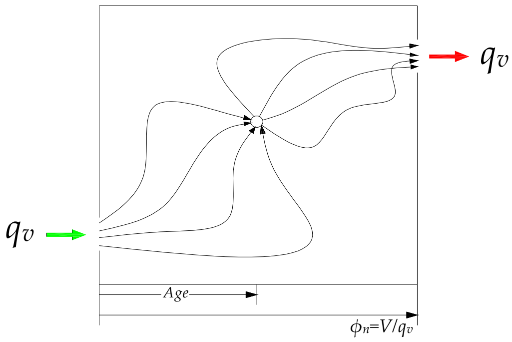

Figure 5. Definition of the age of air [27].

As shown in Figure 5, Age is a nominal time constant which is relevant with the volume V and flux q_V of airflow. The local mean age of air, Φ, is obtained from additional transport equations in the CFD method, which can be formulated as [28]:

$$\mathrm{div}(\Phi\mathbf{U}) = \frac{1}{\rho}\mathrm{div}(\mathrm{Dgrad}\Phi) - \left(\frac{\partial\overline{u'\varphi'}}{\partial x} + \frac{\partial\overline{u'\varphi'}}{\partial y} + \frac{\partial\overline{u'\varphi'}}{\partial z}\right) + 1 \tag{10}$$

where D is the diffusivity of pollutant.

3.3. Boundary Conditions and Solver Settings

The wind speed and wind direction given in Table 1 are regarded as the input conditions of the simulation. According to Prandtl mixing-length theory, the inlet wind speed has an exponential distribution with height [15]:

$$u = u_0\left(\frac{z}{z_0}\right)^a \tag{11}$$

where u is the wind speed at the height z, u_0, the wind speed at the reference height z_0, and a = 0.3 is the constant reflecting the surface roughness in this paper. Therefore, velocity-inlet boundary conditions are input by creating user-defined functions based on Formula (11).

Supposing the outflow has been fully developed and the flow has been restored to normal flow without building obstruction, the relative pressure of the outflow boundary is 0.

SIMPLEC algorithm is employed for coupling pressure and momentum equations. The second-order schemes are used to discretize the convection and diffusion terms. Convergence is achieved when all scaled residuals are less than 10^{-6}.

4. Results and Discussion

4.1. Velocity and Temperature Distribution in the Street Canyon

4.1.1. Velocity Distribution in the Perpendicular Prevailing Wind Direction

In summer, the south-southeast wind prevails and the coming airflow is perpendicular to the street canyon. The contour and vector plot of air velocities are presented in Figure 6. The air velocity is found to distribute unevenly in the whole region. Higher air velocity appears in residential areas and innovative districts located at the edge of the city. The velocity is obviously weakened due to the resistance of high-rise building clusters in the front, as shown in dark blue in Figure 6a. The air velocity distributing in the north direction of the street is less than 1 m/s, while in innovative districts the air velocity is up to 3 m/s. Branches of the main street play an important role in ventilation when the coming wind direction is perpendicular to the street canyon. The city ventilation is enhanced by airflows inside the new urban region, as shown in Figure 6b. The central street then brings the airflow to residential areas along downstream with the air velocity of 1 m/s.

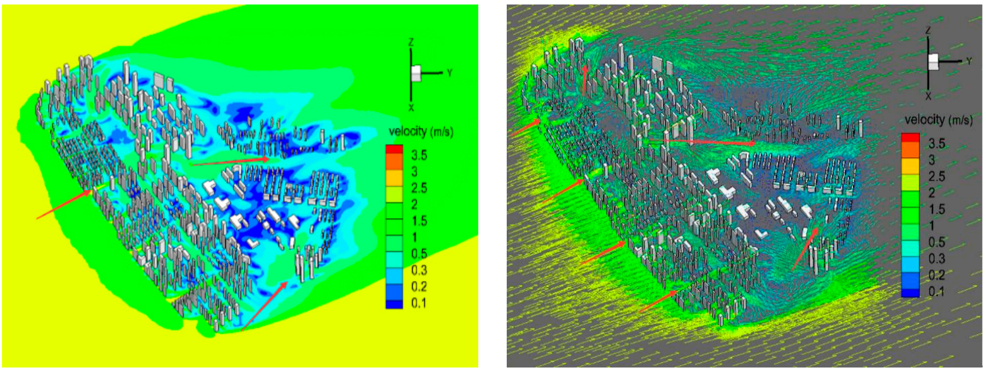

(**a**) (**b**)

Figure 6. Urban wind velocity distribution in summer: (**a**) Contour plot; (**b**) Vector plot.

4.1.2. Velocity Distribution in the Parallel Prevailing Wind Direction

In winter, the east-northeast wind prevails in this city, parallel to the street canyon. The contour and vector plot of the air velocity are illustrated in Figure 7. Results demonstrate that wind stream from ecological areas and open space is mostly induced by the central long street into building clusters and then disperses into dense areas downstream through branches.

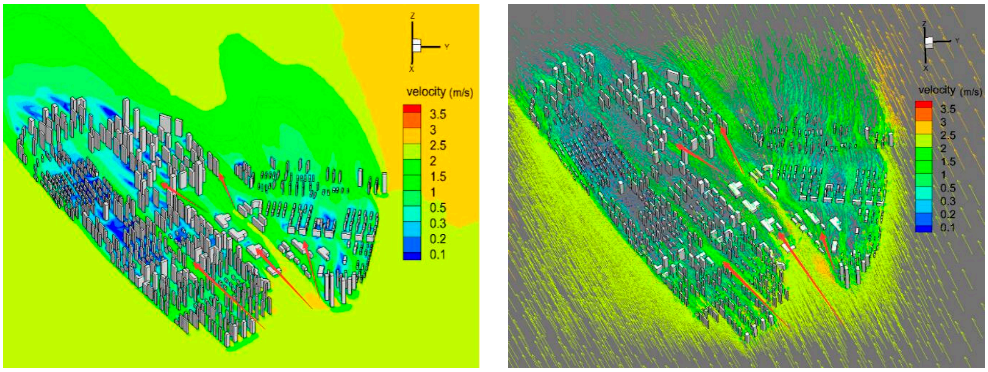

(**a**) (**b**)

Figure 7. Urban wind velocity distribution in winter: (**a**) Contour plot; (**b**) Vector plot.

Figure 7 indicates that the air velocity in the central street ranges from 2 m/s to 2.5 m/s, higher than that in other regions. Different from that in summer, the central street plays the major role in the urban ventilation in winter. What is more, both military and innovative districts are located upwind with a high air velocity so that pollutants produced here will disperse quickly. However, the air velocity decreases in residential areas due to the drag force around high-rise buildings in the front, which means that the high-rise buildings potentially act as windbreaks in winter.

4.1.3. Temperature Distribution on Building Facades under the Ventilation in the Street Canyon

The formation of heat accumulation is strongly closely related to the poor urban ventilation. A well-designed street canyon is not only an energy-saving way to optimize the wind environment, but an effective method to reduce heat accumulations. Among the heat generated from the whole region, the emission from air conditioning systems in densely-populated residential areas, innovative districts, and public service areas on both sides contribute chiefly to the heat accumulation. The main emission is simplified as the body heat source inside each sub-regions. In addition, the significant heat radiation from sunshine in summer is simplified as surface heat source (see Table 2). The inflow is set with the same temperature with near suburbs.

Figure 8 demonstrates air temperature on building facades in the street canyon in summer. The maximum temperature appears near the center of the underlying surface in the region, especially in dense building clusters. A wider range of high temperature appears in the leeward side. It can be seen that the temperature in the southeast (33∼35 °C at windward) is relatively low where the wind flows into the city from open spaces. Because of the low height of buildings, effective ventilation through branches occurs in residential districts and innovative areas, and heat elimination can be easily realized and consequently downgrades the temperature. When the air flows through the central street, the originally emitted heat is reduced greatly due to favorable ventilation. As a result, the temperature in downstream districts decreases, especially in some residential areas. In comparison, airflows diffuse freely without any obstruction, such as buildings around the central street, expelling the heat inside the city quickly and maintaining a low temperature.

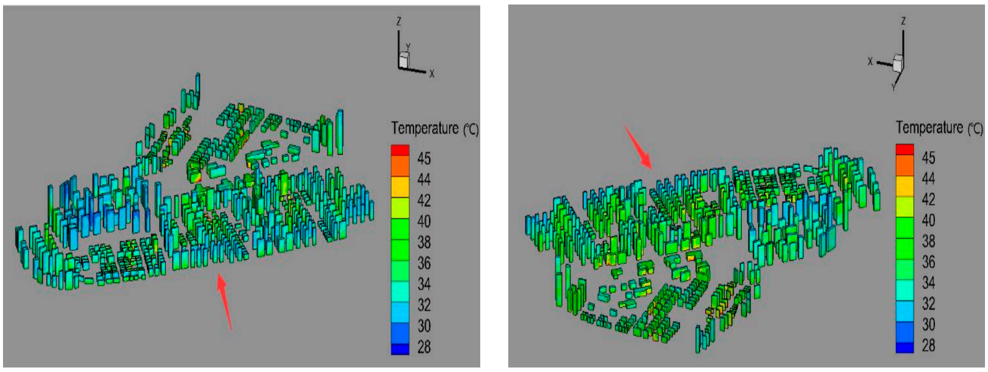

(**a**) (**b**)

Figure 8. Temperature distributions on building façades in summer: (**a**) Windward; (**b**) Leeward.

The vertical variations of temperatures inside the street canyon are calculated and compared under given prevailing wind speeds, as shown in Figure 9.

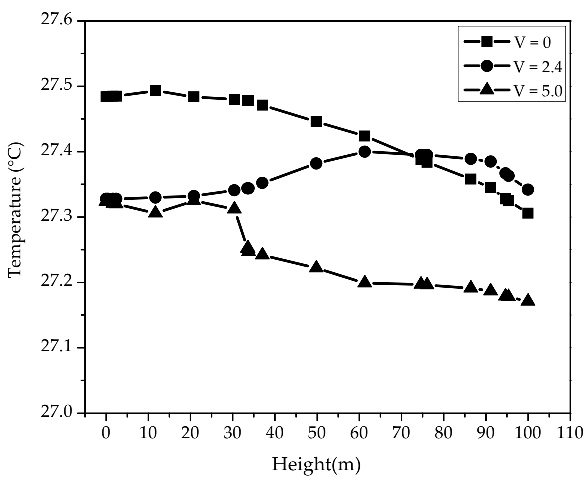

Figure 9. Vertical temperature inside the street canyon (V is the velocity of prevailing wind, $m \cdot s^{-1}$).

It is obviously seen that the temperature in the street canyon varies from wind speeds and height. When the height is lower than 30 m, the temperature varies similarly from height under two coming wind speeds, and keeps smaller values as compared to circumstance without ventilation. Subsequently, a larger the coming wind speed is found to be associated with a lower air temperature, when the height is lower than 80 m, approximately the height of most buildings around the monitored site. When the height is above 80 m, the temperature naturally decreases with height and without ventilation.

Larger airflow ($V > 0$) in the street canyon greatly benefits the removal of the heat inside of the city, which then reduces the local air temperature. Driven by temperature difference, airflows spread from high-temperature areas to low-temperature areas, and the heat can be partially carried away by the convection. The temperature difference near the ground surface (< 30 m) of different airflow is ignorable and larger airflow plays a vital role in higher spaces (30 m $< V <$ 80 m). Besides, the central long street enables cooler and fresher air to be introduced from the suburb area to the central building clusters area, improving the ventilation and weakening the heat accumulation effect in this region.

4.2. Outdoor Wind Speeds and Human Body Comfort

It is reported that the physical environment about 1.5 m above ground affects how a person feels most directly [16]. Therefore, airflow velocity at 1.5 m is employed to assess the ventilation effectiveness in this region. Table 3 illustrates the different comfort levels of the human body at different wind speed levels. Generally, the outdoor wind speed from 1.0 m/s to 5.0 m/s is appreciated to be the most comfortable environment for human outdoors.

Table 3. Wind scales and human body comfort [34].

Wind Scale	Human Body Comfor
<1.0 m/s	Breezeless
1.0∼5.0 m/s	Comfortable
5.0∼10.0 m/s	Uncomfortable with movement affected
10.0∼15.0 m/s	Very uncomfortable with movement greatly affected
15.0∼20.0 m/s	Intolerable
>20.0 m/s	Dangerous

To evaluate the urban ventilation and to compare its effects on human bodies under two prevailing wind directions, wind speeds at the height of 1.5 m in two seasons are calculated, respectively (see Table 4), and analyzed below.

Table 4. The percentage of the wind speed, with the observed minimum and maximum speed values in parentheses.

Velocity (m/s)	Percentage (%)	
	SSE (Summer)	ENE (Winter)
0 (air stagnation)	10.44	5.78
0∼0.5	45.25 (0.04–0.50)	20.17 (0.01–0.50)
0.5∼1.0	18.22 (0.51–0.98)	46.13 (0.51–0.10)
1.0∼3.0	26.09 (1.01–2.89)	27.92 (1.01–2.78)

Results show that the air stagnation in the whole region occupies 10.44% in summer, larger than 5.78% in winter, which means that worse air circulation occurs more easily when the prevailing wind is perpendicular to the street canyon. In winter, compared with street branches, the central long street brings better airflows. Moreover, the velocity varying within 0∼0.5 m/s in summer accounts for 45.25%, considerably larger than the percentage (20.17%) in winter while the proportion of the velocity within 0.5∼1.0 m/s in summer (18.2%) is greatly lower than that in winter (46.13%). This further emphasizes relatively worse ventilations induced by when the coming wind is perpendicular to the street canyon. On the contrary, the prevailing wind direction parallel to the street canyon easily accelerate airflows, especially inside building clusters. It is interesting to note from the data in Table 2 that the velocity in summer ranging from 1.0 m/s to 3.0 m/s constitutes 26.09%, which is similar to the percentage 27.92% in winter. In respect to wind velocity, little comfort difference is found for human body between the prevailing wind direction of perpendicular or parallel to the street canyon.

From the perspective of human body comfort, the ventilation conditions are shown to be favorable in both patterns in the street canyon where the central long street dominates the whole wind field, especially when the wind comes from its parallel direction. When the wind direction is perpendicular to the street canyon, the combination of branches of the street also effectively promotes the ventilation. However, air stagnation occurs more easily in the street canyon under the perpendicular wind, leading to adverse contaminant accumulation.

4.3. Wind Pressure on Building Envelopes

Natural ventilation is driven by the wind pressure difference and the temperature difference in air [35]. When the temperature difference between the indoor and outdoor environment is too small to provide drive force, the natural ventilation needs to rely on the wind pressure on building envelopes [36]. The natural ventilation is formed when the wind pressures differences exist on both sides of certain openings (i.e., all kinds of holes, doors, windows, and gaps). The outdoors pressure difference also determines the indoor ventilation effectiveness, as greater pressure difference providing more favorable ventilation.

The flux of airflow through openings can be calculated by Bernoulli equation [37]:

$$Q = \alpha A \sqrt{\frac{2\Delta p}{\rho}} \tag{12}$$

The flux of airflow has an increase tendency with the increase of pressure on building surfaces, while the atmospheric pressure maintains a constant P_0. Here, convert the surface pressure to dimensionless ones, the coefficient of wind-pressure C_p can be derived as:

$$C_p = \frac{P_0}{\rho v^2/2} \tag{13}$$

where ρ is air density and v is airflow velocity.

The distribution of coefficients of wind pressure is shown in Figure 10. Large coefficients $(C_p > 1)$ generally appear on the windward side of high-rise buildings and the lower reaches of the street canyon. In these areas, the pressure on building envelopes is higher than that of atmospheric pressure, which contributes to the airflow circulation from the street canyon to the suburbs. Besides, large pressure on building facades can achieve a favorable ventilation for indoor individuals. Conversely, in these areas with low pressure coefficients $(C_p < 1)$, little pressure difference between forward and backward of buildings has a critical influence on the formation of shade of wind, followed by the contaminant accumulation in the street canyon. Meanwhile, for indoor dwellers, the reasonable interior arrangement, apartment layout, and window installation are suggested to make a good ventilation.

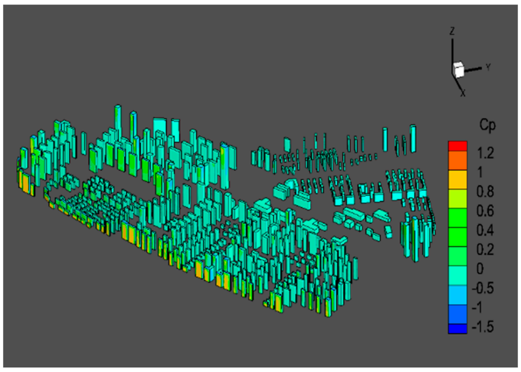

Figure 10. Coefficients of wind pressure.

4.4. Air-Age-Based Discussions on the "Freshness" of Outdoor Air

The air age in the street canyon is used to evaluate the "freshness" of outdoor air and lower values suggest fresher air. The boundary conditions for the air age governing equation are 0 at the air inlet, and the gradient is 0 in both the air exit and the wall surfaces of the computational domain.

Figure 11 shows the calculative air age and its corresponding air velocity. It is obviously seen that the maximum ages (4000∼6000 s) appear in military districts where it is difficult for fresh air to flow into due to its poor ventilation. Similarly, in those areas perpendicular to the coming wind and spaces among high-rise buildings in innovative districts and residential areas, larger air age and lower velocity is found (see Figure 11b). In lower reaches of innovative districts and leeside of military districts, where air velocities are mostly lower than 0.2 m/s, the local maximum of air age is up to 7000 s. Low air ages (< 3000 s) distribute in most part of this region, mainly in residential areas and innovative streets and gets older along downstream gradually. Relatively high air velocities appear in the streets that are parallel to the direction of the wind, indicating promising ventilation and quick air exchange in those. Derived data illustrates that the ages of air in the street canyon are mostly twice the minimum values in upstream of residential areas and innovative streets. In military districts and some downstream building clusters, the age of air becomes larger with a local maximum of up to 3 times larger than the minimum. Correspondingly, fresher air exists in most parts of this region and older air only distributes in local districts with poor ventilation, especially in downstream regions behind dense buildings.

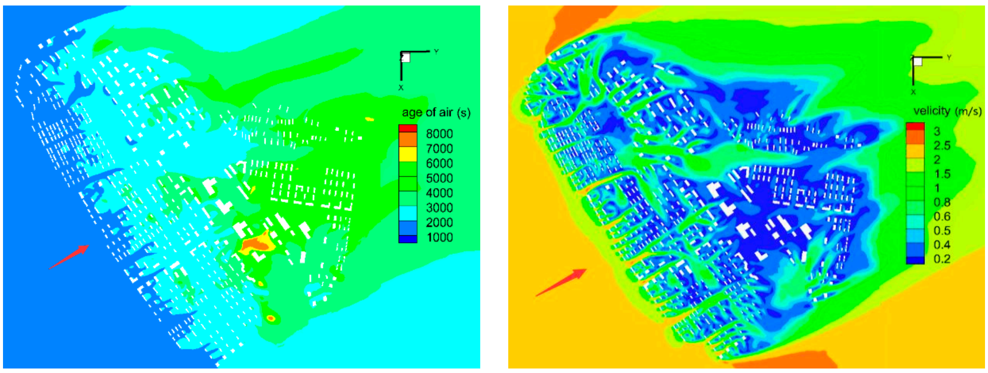

(**a**) (**b**)

Figure 11. Stagnation of air in the Southern New City region in summer: (**a**) Age of air; (**b**) Airflow velocity.

5. Conclusions

Based on the planned Southern New Town region in Nanjing, China, this study focused on the microclimate and pollutant dispersion in urban street canyons under two typical seasons (i.e., summer and winter). The flow field, temperature field, and the age of air were calculated with the CFD method and analyzed under two typical prevailing winds. Results revealed that there was little comfort difference for the human body between the prevailing wind direction of perpendicular or parallel to the street canyon. Air stagnation occurred easily in dense building clusters, especially under the perpendicular wind direction. In addition, large pressure coefficients ($C_P > 1$) appeared at the windward region, contributing to the promising ventilation. The air age was introduced to evaluate the "freshness" of the air in the street canyon and illustrate the ventilation effectiveness on the pollutant removal. It was found that the air was updated easily where the ventilation was favorable and wind speed was large.

Following conclusions were to be drawn:

(1) The planned region was basically well-ventilated whether the coming wind direction was parallel or perpendicular to the street canyon. However, the air stagnation easily occurred in summer when the prevailing wind was perpendicular to the street canyon.
(2) The favorable ventilation comfort appeared both patterns in the street canyon where the central long street dominated the whole wind field, especially when the wind came from its parallel direction.
(3) Pressure coefficients indicated that the outdoor wind environment for building clusters located at the upper reaches were more favorable than those in lower reaches of the coming wind.
(4) The age of air showed that the poor ventilation will cause the old air detained and make it difficult to exchange the fresh air, resulting in bad air quality in the street canyon, especially in downstream regions behind dense buildings.

However, there are still limitations in field measurements to improve on the study of street canyons in this region, and the wind environment in the area outside the street canyon is worth discussing and studying.

Acknowledgments: We sincerely appreciate the financial supported by the National Key Research and Development Program of China 2016YFC0700500.

Author Contributions: Fan Liu and Hua Qian conceived and designed the research content; Xiaohong Zheng, Lun Zhang and Wenqing Liang collected the data; Fan Liu analyzed the data; Hua Qian contributed to the discussion of data analysis; Fan Liu wrote the paper.

Conflicts of Interest: The authors declare no conflict of interest.

References

1. Fernando, H.J.S.; Lee, S.M.; Anderson, J.; Princevac, M.; Pardyjak, E.; Grossman-Clarke, S. Urban Fluid Mechanics: Air Circulation and Contaminant Dispersion in Cities. *Environ. Fluid Mech.* **2001**, *1*, 107–164. [CrossRef]
2. Huang, Y.D.; He, W.R.; Kim, C.N. Impacts of shape and height of upstream roof on airflow and pollutant dispersion inside an urban street canyon. *Environ. Sci. Pollut.* **2014**, *22*, 2117–2137. [CrossRef] [PubMed]
3. Kwak, K.H.; Baik, J.J.; Lee, K.Y. Dispersion and photochemical evolution of reactive pollutants in street canyons. *Atmos. Environ.* **2013**, *70*, 98–107. [CrossRef]
4. Baklanov, A.; Molina, L.T.; Gauss, M. Megacities, air quality and climate. *Atmos. Environ.* **2016**, *126*, 235–249. [CrossRef]
5. Jin, X.; Yang, L.; Du, X.; Yang, Y. Particle transport characteristics in the micro-environment near the roadway. *Build. Environ.* **2016**, *102*, 138–158. [CrossRef]
6. Hsieh, C.M.; Huang, H.C. Mitigating urban heat islands: A method to identify potential wind corridor for cooling and ventilation. *Comput. Environ. Urban* **2016**, *57*, 130–143. [CrossRef]

7. Takebayashi, H.; Moriyama, M. Relationships between the properties of an urban street canyon and its radiant environment: Introduction of appropriate urban heat island mitigation technologies. *Sol. Energy* **2012**, *86*, 2255–2262. [CrossRef]
8. Giridharan, R.; Ganesan, S.; Lau, S.S.Y. Daytime urban heat island effect in high-rise and high-density residential developments in Hong Kong. *Energy Build.* **2004**, *36*, 525–534. [CrossRef]
9. Georgakis, C.; Zoras, S.; Santamouris, M. Studying the effect of "cool" coatings in street urban canyons and its potential as a heat island mitigation technique. *Sustain. Cities Soc.* **2014**, *13*, 20–31. [CrossRef]
10. Mei, S.J.; Liu, C.W.; Liu, D.; Zhao, F.Y.; Wang, H.Q.; Li, X.H. Fluid mechanical dispersion of airborne pollutants inside urban street canyons subjecting to multi-component ventilation and unstable thermal stratifications. *Sci. Total Environ.* **2016**, *565*, 1102–1115. [CrossRef] [PubMed]
11. Li, S.S.; Williams, G.; Guo, Y.M. Health benefits from improved outdoor air quality and intervention in China. *Environ. Pollut.* **2016**, *214*, 17–25. [CrossRef] [PubMed]
12. Liu, J.L.; Niu, J.L. CFD simulation of the wind environment around an isolated high-rise building: An evaluation of SRANS, LES and DES models. *Build. Environ.* **2016**, *96*, 91–106. [CrossRef]
13. Yoshie, R.; Mochida, A.; Tominaga, Y.; Kataoka, H.; Harimoto, K.; Nozu, T.; Shirasawa, T. Cooperative project for CFD prediction of pedestrian wind environment in the architectural institute of Japan. *J. Wind Eng. Ind. Aerodyn.* **2007**, *95*, 1551–1578. [CrossRef]
14. Ricci, A.; Burlando, M.; Freda, A.; Repetto, M.P. Wind tunnel measurements of the urban boundary layer development over a historical district in Italy. *Build. Environ.* **2017**, *111*, 192–206. [CrossRef]
15. Tominaga, Y.; Mochida, A.; Yoshie, R.; Kataoka, H.; Nozu, T.; Yoshikawa, M.; Shirasawa, T. AIJ guidelines for practical applications of CFD to pedestrian wind environment around buildings. *J. Wind Eng. Ind. Aerodyn.* **2008**, *96*, 1749–1761. [CrossRef]
16. Ramponi, R.; Blocken, B.; de Cooa, L.B.; Janssen, W.D. CFD simulation of outdoor ventilation of generic urban configurations with different urban densities and equal and unequal street widths. *Build. Environ.* **2015**, *92*, 152–166. [CrossRef]
17. Tong, Z.M.; Chen, Y.J.; Malkawi, A. Defining the Influence Region in neighborhood-scale CFD simulations for natural ventilation design. *Appl. Energy* **2016**, *182*, 625–633. [CrossRef]
18. Blocken, B.; Janssen, W.D.; van Hooff, T. CFD simulation for pedestrian wind comfort and wind safety in urban areas: General decision framework and case study for the Eindhoven University campus. *Environ. Model. Softw.* **2012**, *30*, 15–34. [CrossRef]
19. He, L.J.; Hang, J.; Wang, X.M.; Lin, B.R.; Li, X.H.; Lan, G.D. Numerical investigations of flow and passive pollutant exposure inhigh-rise deep street canyons with various street aspect ratios and viaduct settings. *Sci. Total Environ.* **2017**, *584–585*, 189–206. [CrossRef] [PubMed]
20. Yang, F.; Gao, Y.W.; Zhong, K.; Kang, Y.M. Impacts of cross-ventilation on the air quality in street canyons with different building arrangements. *Build. Environ.* **2016**, *104*, 1–12. [CrossRef]
21. Chatzidimitriou, A.; Yannas, S. Street canyon design and improvement potential for urban open spaces; the influence of canyon aspect ratio and orientation on microclimate and outdoor comfort. *Sustain. Cities Soc.* **2017**, *33*, 85–101. [CrossRef]
22. Perret, L.; Blackman, K.; Fernandes, R.; Savory, E. Relating street canyon vertical mass-exchange to upstream flow regime and canyon geometry. *Sustain. Cities Soc.* **2017**, *30*, 49–57. [CrossRef]
23. Tominaga, Y.; Stathopoulos, T. CFD modeling of pollution dispersion in a street canyon: Comparison between LES and RANS. *J. Wind Eng. Ind. Aerodyn.* **2011**, *99*, 340–348. [CrossRef]
24. Park, S.J.; Choi, W.; Kim, J.J.; Kim, M.J.; Park, R.J.; Han, K.S.; Kang, G. Effects of building-roof cooling on the flow and dispersion of reactive pollutants in an idealized urban street canyon. *Build. Environ.* **2016**, *109*, 175–189. [CrossRef]
25. Ai, Z.T.; Mak, C.M. CFD simulation of flow in a long street canyon under a perpendicular wind direction: Evaluation of three computational settings. *Build. Environ.* **2016**, *114*, 293–306. [CrossRef]
26. Sandberg, M. What is ventilation efficiency? *Build. Environ.* **1981**, *16*, 123–135.
27. Etherldge, D.; Sandberg, M. *Building Ventilation: Theory and Measurement*; John Wiley & Sons: Chichester, UK, 1996.
28. Hang, J.; Sandberg, M.; Li, Y.G. Age of air and air exchange efficiency in idealized city models. *Build. Environ.* **2009**, *44*, 1714–1723. [CrossRef]

29. Hang, J.; Li, Y.G. Age of air and air exchange efficiency in high-rise urban areas and its link to pollutant dilution. *Atmos. Environ.* **2011**, *45*, 5572–5585. [CrossRef]
30. Mochida, A.; Tominaga, Y.; Murakami, S.; Yoshie, R.; Ishihara, T.; Ooka, R. Comparison of various k–emodels and DSM applied to flow around a high-rise building—Report on AIJ cooperative project for CFD prediction of wind environment. *Wind Struct.* **2002**, *5*, 227–244. [CrossRef]
31. Versteeg, H.K.; Malalasekera, W. *An Introduction to Computational Fluid Dynamics: The Finite Volume Method*, 2nd ed.; Beijing World Publishing Corporation: Beijing, China, 2007; pp. 87–88.
32. Yakhot, V.; Orszag, S.A.; Thangam, S.; Gatski, T.B.; Speziale, C.G. Development of turbulence models for shear flows by a doble expansion technique. *Phys. Fluids A* **1992**, *4*, 1510–1520. [CrossRef]
33. Yakhot, V.; Orszag, S.A. Renormalization-group analysis of turbulence. *Phys. Rev. Lett.* **1986**, *57*, 6396–6409. [CrossRef] [PubMed]
34. Sini, J.F.; Anquetin, S.; Mestayer, P.G. Pollutant dispersion and thermal effects in urban street canyons. *Atmos. Environ.* **1996**, *30*, 2659–2677. [CrossRef]
35. Burnett, J.; Bojic, M.; Yik, F. Wind-induced pressure at external surfaces of a high-rise residential building in Hong Kong. *Build. Environ.* **2005**, *40*, 765–777. [CrossRef]
36. Yuan, C.S. The effect of building shape modification on wind pressure differences for cross-ventilation of a low-rise building. *Int. J. Vent.* **2007**, *6*, 167–176. [CrossRef]
37. Kelley, J.B. The extended Bernoulli equation. *Am. J. Phys.* **1950**, *18*, 202–204. [CrossRef]